Journal of Global Science ISSN: 2453-756X (online) http://www.jogsc.com

The employment of force in the duty cycle of variable wing geometry technology

Ing. Branislav Rácek, PhD.
Technical University of Kosice
Department of Aviation Engineering
Rampová 7, 041 21 KOSICE
branislav.racek@tuke.sk

doc. Ing. Michal Hovanec, PhD., Ing.Paed.IGIP
Technical University of Kosice
Department of Aviation Engineering
Rampová 7, 041 21 KOSICE
michal.hovanec@tuke.sk

Ing. Maroš Divok , PhD.
Technical University of Kosice
Department of Aviation Engineering
Rampová 7, 041 21 KOSICE
maros.divok@tuke.sk

Ing. Samer AL-RABEEI , PhD.*
Technical University of Kosice
Department of Aviation Engineering
Rampová 7, 041 21 KOSICE
Samer.al-rabeei@tuke.sk

Ing. Volodymyr Tymofiiv, PhD.
Technical University of Kosice
Department of Aviation Engineering
Rampová 7, 041 21 KOSICE
volodymir.tymofiiv@tuke.sk

Abstract
The present paper examines the force action in the duty cycle of variable geometry airfoils (VGK), with a particular focus on shear forces, bending and torsional moments in the wing root region. The half-wing model is formulated as a beam with a fixed heel, with continuous aerodynamic loading, while three representative modes of adjustable camber (S1–S3) are compared. Absent any intention of employing particular numerical values, the present study offers generalised equations and normalised relations that facilitate the dimensional assessment of the root nodes and the adjustment mechanism. The discussion

encompasses the displacement of the lift action point relative to the elastic axis, the mass contribution of the mechanism, and the nature of critical transition states. The results have been formulated in such a manner that they are applicable to a variety of configurations without being tied to a specific aircraft type.

Keywords
variable wing geometry, thrust force, bending moment, torsional moment, sweep angle, aeroelasticity.

Acknowledgement
This work was supported by the KEGA project “Economic assessments of the negative impact of aircraft noise and harmful emissions produced by aircraft engines,” project No. 044TUKE-4/2025, carried out at the Technical University of Košice. The authors gratefully acknowledge this support.

1. • b — wingspan; a half-wing is considered in the interval y ∈ [0, b/2]
2. • c(y) — local profile depth
3. • x_ac — position of the aerodynamic center (≈ 0.25 c)
4. • x_cp(y) — position of the resultant lift (center of aerodynamic pressure)
5. • x_ea(y) — position of the elastic axis
6. • ρ — air density, V — flight speed, n — overload factor
7. • C_L(y,Λ) — local lift coefficient taking into account sweep angle Λ
8. • q(y) — continuous surface load [N/m] acting perpendicular to the reference plane
9. • V(y) — shear force [N]
10. • M(y) — bending moment [N·m]
11. • t(y) — torsional moment density [N]·m/m; T(y) — torsional moment [N·m]

Introduction

In aviation practice, we encounter many unusual design solutions that seek to enrich the world of aviation and at the same time bring functional use in operation. One such significant elements, which has entered the history of aviation thanks to a specific spectrum of flight characteristics, is the variable geometry of the airfoils (VGK), often understood as an adjustable wing sweep. Its essence is to allow the aircraft to approach the "ideal" wing for different flight modes: at low speeds with high load capacity and good manoeuvrability, and at high speeds with low resistance and sufficient aeroelastic reserve [1]. Such a concept brings obvious aerodynamic benefits but at the same time significantly increases the demands on the design, propulsion and integrity of the support system. The camber adjustment mechanism (pins, bearings, locks and actuators) must safely transmit sliding forces, bending and torques throughout the entire adjustment cycle. Changing the geometry also changes the position of the aerodynamic centre of gravity and the distribution of the continuous load along the span, which affects the V(y) and M(y) curves, local stresses in the root area and fatigue design. Added to these effects is the weight gain of the mechanism itself and its location relative to the elastic axis, which can reduce torsional stiffness and affect the reserves against vibration and flutter [2]. The aim of this work is to quantify the force action in the VGK duty cycle and to show how the key internal forces and moments in the wing change under typical operating conditions. We start from a simple, but for design considerations sufficient, model of a half-wing as a beam with a fixed root, which is subjected to a continuous aerodynamic load approximated by the local profile depth and lift coefficient. For selected

camber positions, we compare the nominal V(y), M(y) and torsional effects with respect to the elastic axis, especially with respect to the root support and the locks of the adjustment mechanism. We also discuss the impacts on the dimensioning of the ribbing and skin in the root area and on the cyclic stress resulting from repeated adjustments in service [3].

1. Basic theoretical principles

During steady straight flight, the weight of the aircraft is balanced by lift, so Y = G. However, the aircraft does not fly in a straight line for its entire length. In addition to performing various flight tasks, flight operations also include a wide variety of manoeuvres in which the aircraft moves with greater or lesser acceleration. The value of acceleration depends on various flight parameters, such as the type of manoeuvre performed, the flight speed at which the manoeuvre is performed, and the flight path parameters. The effect of acceleration is introduced into the load calculations by means of a multiplier n, whose maximum permissible value depends not only on the individual types and categories of aircraft but also varies for the individual structural parts of the airframe defined in the strength regulations. For flights with acceleration, the wing load is determined by the equation Y = n.G. Since the multiplier n only covers load values associated with flight operations, a safety factor f is also used in the equation, which ranges between f = 1.5-2 for the wing. The lift force acting on the wing thus has the character of a numerical load, and the equation will be given in the form [4]:

$$Y_{poč} = n * G * f \quad (1).$$

For the design of the main load-bearing elements of the wing, it is necessary to distribute the effect of lift force continuously over both the span and the depth of the wing. Knowledge of the load distribution across the wingspan allows the values of shear forces and bending moments in each section of the wing to be determined, while the load distribution across the depth of the profile is important mainly for determining the effects of torsional moments. The distribution of continuous aerodynamic load depends on the value of the local lift coefficient, which varies across the span. With a minimum degree of inaccuracy, it can be assumed that the value of the local lift coefficient is constant and equal to the lift coefficient of the wing. The continuous load in any section of the wing will then depend only on the local wing depth b and will be expressed by the equation:

[1]

$$q_y = \frac{n * G * f}{S_{krídla}} * b$$

The effect of aerodynamic forces on the wing depth can be determined from the moment equilibrium with respect to the leading edge of the wing profile. In conventional designs intended for subsonic flight speeds and low angles of attack, it is located at a distance of approximately 25% from the leading edge of the wing. To obtain strength calculations for the wing, it is often important to convert the applied load to a load acting in a plane perpendicular to the chord c_n and in the chord plane c_t. These conversions are particularly important for flight modes where the aircraft is moving at high angles of attack. The conversion can be performed according to Figure 1 using equations [4].

$$c_n = c_y * cos \propto + c_x * sin \propto$$
$$c_t = c_x * cos \propto - c_y * sin \propto$$

In a similar way, it is then possible to create transfer equations for continuous loads q.

$$q_n = q_y * cos \propto + q_x * sin \propto$$
$$q_t = q_x * cos \propto - q_y * sin \propto$$

At small angles of attack, when the value of sin α approaches zero and cos α approaches 1, it can be assumed that q_n=q_y and q_t=q_x [4].

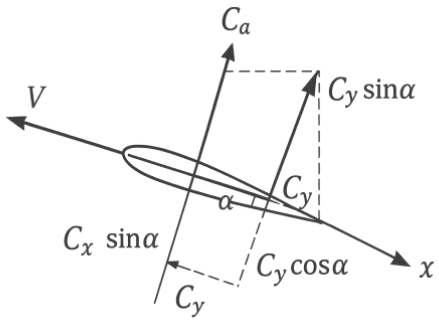

Figure 1 Decomposition of aerodynamic forces/coefficients at angle of attack

1.1 Influence of loads from weight forces

When calculating the distribution of loads from weight forces, the same simplifying assumptions can be used as in the previous case, i.e. that the continuous load on the span is proportional to the local depths of the wing in individual sections. The following equation can then be used:

[4]

$$q_{mkrídla} = \frac{n * G_{krídla} * f}{S_{krídla}} * b$$

In this equation, G_wing is the weight of the wing and b is the local depth of the wing section. If more detailed data on the weight of different sections of the wing are not available, it is necessary to introduce the exponent m = 2-3 for a more accurate calculation, which serves to introduce the influence of the type of construction into the solution. The equation will then take the following form:

[4]

$$q_{mkrídla} = \frac{n * G_{krídla} * f}{S_{krídla}} * b^m$$

The center of gravity of the weight forces is located at the center of gravity of the given section, and in a conventional wing it lies at 40-50% of its depth. Knowledge of this type of load and its point of application is essential not only for static calculations, but also in view of the possibility of aeroelastic phenomena, which are very dangerous for the structures of individual aircraft parts [4].

2. Models and methods

The half-wing is considered as a space beam with a fixed base in the root region and a free end at y = b/2. The load is represented by a continuous aerodynamic distribution q(y), supplemented by the mass effects of the self-mass and the VGK mechanism. For the longitudinal coordinate, we use the y-axis from the root (y = 0) to the end of the half-wing (y = b/2). The boundary conditions are V(b/2) = 0 and M(b/2) = 0.
The local profile depth is approximated by a linear function with taper ratio λ = c_tip/c_root [5]:
$c(y) = c_{root} \cdot [\, 1 - (1 - \lambda) \cdot (2y/b) \,]$
The effect of the camber Λ is included by the multiplicative coefficient $k_L(\Lambda) \in (0, 1]$, which takes into account the effective reduction of the lift derivative in oblique blowing [6].

Continuous aerodynamic load:
$q(y) = \frac{1}{2} \cdot \rho \cdot V^2 \cdot n \cdot c(y) \cdot C_L(y, \Lambda)$
Equations of equilibrium (with negative derivative according to the usual convention dV/dy = −q, dM/dy = V):
$V(y) = \int_{y}^{b/2} q(\xi)\, d\xi$
$M(y) = \int_{y}^{b/2} V(\xi)\, d\xi$
Torsion effects with respect to the elastic axis (x_ea):
$t(y) = q(y) \cdot [\, x_{cp}(y) - x_{ea}(y) \,]$
$T_{root} = \int_{0}^{b/2} t(y)\, dy$
Normalization for mode comparison:
$\tilde{V}(y) = V(y) / V(0)|_{S1}$, $\tilde{M}(y) = M(y) / M(0)|_{S1}$, $\tilde{T}_{root} = T_{root} / T_{root}|_{S1}$ [7]

3. Variable geometry swashplate modes

• S1 — low camber (e.g. takeoffs and approaches), increased lift capacity (n > 1). The load distribution is closer to elliptical; we assume larger C_L and smaller k_L(Λ).
• S2 — medium camber (transition phases), nominal n ≈ 1. Balanced compromise between drag and lift capacity; C_L and k_L(Λ) have intermediate values.
• S3 — high camber (fast/cruise flight), lower induced wingtip loads; k_L(Λ) is smaller, but at higher V aerodynamic loads are applied and the position of x_cp changes.

4. Discussion

4.1 Internal force and moment curves. For all evaluated modes, the root bending moment M(0) dominates. At low camber (S1), higher C_L leads to higher values of ~M(0), but the curve is more favourable in terms of load uniformity. At high camber (S3), the lift action point shifts backward and towards the root, which decreases ~M(0) with respect to S1, but the torsional component increases. The shear force V(y) remains monotonic with zero at the wing tip; changes in pitch reflect local variations in q(y).
4.2 Torsional effects and the elastic axis. Torsional effects are controlled by the difference [x_cp(y) − x_ea(y)]. When adjusting to a larger camber, an increase in ~T_root may occur even with an unchanged M(0), especially if the masses of the mechanism lie outside the elastic axis. Therefore, minimizing the eccentricity of the actuators and appropriately dimensioning the casing/stands is critical.

4.3 Transient states and fatigue considerations. The highest combined stresses typically occur during the resetting, when k_L(Λ) and x_cp(y) change and the mechanism overcomes the locks. It is recommended to work with design spectra including the transitions S1→S2→S3 and back, and to control the resetting speed in areas with high T_root increase.
4.4 Implications for design and maintenance. The results indicate a requirement for eccentricity control, increasing the torsional stiffness in the root region, introducing limits on the resetting dynamics, and targeted NDT checks of the pins/bearings according to monitored clearance and vibration trends.
4.5 Limits of access. The presented relationships do not include fully coupled aeroelasticity or lock nonlinearities; they serve as a conservative basis. If numerical inputs are available, extension with 3D FEM and comparison with tunnel or flight measurements is appropriate.

5. Conclusion

Variable geometry wing designs have been used only to a limited extent, despite their ability to expand the spectrum of operating modes. Their higher complexity, weight gain and maintenance requirements, combined with the enormous stress on the rotating mechanisms, pose significant risks in terms of reliability and life costs. In the civil operation environment, which is today set to maximise aircraft availability and minimize costs per seat-kilometre, simpler and more reliable solutions generally prevail.
Computational considerations in this work have shown that during the adjustment of the sweep, unfavourable combinations of shear forces, bending and torsional moments arise in the wing root area and in the mechanism itself. Particularly critical are the bending moment peaks during transitions between modes and torsional effects with respect to the elastic axis, which accelerate the fatigue of pins, bearings and locks. Practical aspects are also added – seals and mechanism covers increase complex drag, aerodynamic centre of gravity shifts complicate balancing, and certification requires conservative safety factors.
From an aircraft architecture perspective, today, much of the benefits of VGK are being taken over by lower-risk alternatives: optimized transonic profiles, high-efficiency flaps and slots, adaptive/variable flaps (variable camber), composite “elastic tailoring”, controlled load relief, and precise fly-by-wire. These approaches bring similar benefits in typical flight phases without significantly penalising reliability and maintenance.
Three recommendations emerge for practice:

1. Design – minimize the eccentricity of the mechanism relative to the elastic axis, consistently address the transfer of torsional flows, and eliminate play in the locks; take into account especially transient states.
2. Verification – focus fatigue calculations and tests on root nodes, pins, and bearings; work with conservative reconfiguration spectra.
3. Operation – implement targeted NDT intervals and vibration/backlash trend monitoring; limit reconfiguration outside of intended flight modes.

Variable geometry thus remains a technically elegant but specialized solution. In the civil segment, the cost-benefit ratio will continue to prevent its wider adoption; however, in specific missions with extreme requirements on the flight envelope, it remains a legitimate option – at the cost of more rigorous design, rigorous validation and disciplined operation.

Reference

1. History of Aircraft & Aviation. (2022). In History of aircraft & aviation. https://doi.org/10.15394/eaglepub.2022.1066.n2
2. Ramsey, J. K. (2006). NASA Aeroelasticity Handbook Volume 2: Design Guides Part 2. NASA Aeroelasticity Handbook Volume 2: Design Guides Part 2. https://ntrs.nasa.gov/api/citations/20070008370/downloads/20070008370.pdfKossinets, Gueorgi, and Duncan J. Watts. 2009. “Origins of Homophily in an Evolving Social Network.” *American Journal of Sociology* 115:405–50. Accessed February 28, 2010. doi:10.1086/599247.
3. Filippone, A. (2012). Advanced aircraft flight performance. https://doi.org/10.1017/cbo9781139161893Weinstein, Joshua I. 2009. “The Market in Plato’s Republic.” *Classical Philology* 104:439–58.
4. Easy Access Rules for Large Aeroplanes (CS-25) - Revision from January 2023 | EASA. (2023, January 30). EASA. https://www.easa.europa.eu/en/document-library/easy-access-rules/online-publications/easy-access-rules-large-aeroplanes-cs-25?page=26
5. Thiede, P. (2001). Aerodynamic Drag Reduction Technologies. In Springer eBooks. https://doi.org/10.1007/978-3-540-45359-8
6. Traub, L. W. (2000b). Aerodynamic characteristics of spanwise cambered Delta wings. Journal of Aircraft, 37(4), 714–724. https://doi.org/10.2514/2.2657
7. Watanabe, Y. (2022). Dynamics of water surface flows and waves. https://doi.org/10.1201/9781003140160